

Constrained Optimization with Energy-Minimizing Curves and Curve Networks — A Survey

Michael Hofer*
Vienna University of Technology

Abstract

We survey recent research results in constrained optimization with curves and curve networks. The addressed topics include constrained variational curve and curve network design, variational motion design, and guaranteed error bound approximation of point cloud data with curve networks. The main theoretic results are summarized with a focus on geometric solutions of the studied problems. A variety of applications is outlined including obstacle avoiding rigid body motion design and smoothing of digital terrain elevation data.

CR Categories: I.3.5 [Computer Graphics]: Computational Geometry and Object Modeling—Geometric algorithms, languages, and systems; Curve, surface, solid, and object representations;

Keywords: curves on surfaces, variational design, constrained optimization, splines, curve networks, interpolation, approximation.

1 Introduction

Curves and curve networks are fundamental for many modeling purposes. Due to the ever increasing number of geometric 3D data that becomes available there is a rising need for curves and curve networks that meet various constraints. The constraints include on surface constraints, tolerance zones that need to be met, and special curves and curve networks that are optimized towards a specific application. There is a multitude of applications that benefit from such tools, ranging from computational anatomy via geosciences to architecture and many more.

In the present paper we survey recent progress that was made in constrained optimization with curves and curve networks. We summarize the most important results and cite relevant papers in the field. We start in Section 2 with geodesics and their computation on various surface representations. In Section 3 we study energy-minimizing spline curves on surfaces and their applications. One of these applications is variational motion design (in the presence of obstacles) which is discussed in Section 4. The generalization of the curve case to the curve network case leads to so-called fair webs presented in Section 5. Their discrete realization has a variety of applications including fair remeshing and constrained smoothing of digital terrain elevation data with prescribed error bounds. We conclude the paper in Section 6 with an outlook towards future research.

*e-mail: hofer@geometrie.tuwien.ac.at, <http://dmg.tuwien.ac.at/hofer>

2 Geodesics

Geodesics on a surface are the generalization of straight lines in the plane. They can not only be defined as the *shortest* curves but e.g. also as the *frontal* or *straightest* curves (see e.g. [Hilbert and Cohn-Vossen 1932] page 194 for an intuitive explanation). Note that on polyhedral (i.e., piecewise linear) surfaces, *shortest* geodesics are not always *straightest* geodesics [Polthier and Schmies 1998]. Nevertheless, straightest geodesics are not always defined between pairs of points on a triangle mesh and are thus not suited for many applications.

The geometric properties of geodesics have been investigated in classical differential geometry (see e.g. [do Carmo 1976]). Geodesic curves can be characterized by the fact that the osculating plane of the curve shall always pass through the surface normal in the curve point. Geodesics in a scaled arc length parameterization also arise as minimizers of the L^2 norm of the first derivative (see e.g. [Pottmann and Hofer 2005]): Let Φ be an m -dimensional surface in Euclidean \mathbb{R}^n , $m < n$. Moreover two points $\mathbf{p}_i \in \Phi, i = 1, 2$ and real numbers $u_1 < u_2$ are given. Among all curves $\mathbf{x} : I = [u_1, u_2] \rightarrow \Phi$ which interpolate the given data, i.e., $\mathbf{x}(u_1) = \mathbf{p}_1$ and $\mathbf{x}(u_2) = \mathbf{p}_2$, a curve \mathbf{c} which minimizes the functional

$$E_1(\mathbf{x}) = \int_{u_1}^{u_2} \|\dot{\mathbf{x}}(u)\|^2 du \quad (1)$$

is a geodesic in a scaled arc length parameterization. We find that the curve's second derivative vectors $\ddot{\mathbf{c}}$ are orthogonal to Φ . In particular, $\dot{\mathbf{c}}$ and $\ddot{\mathbf{c}}$ are orthogonal, and hence $\|\dot{\mathbf{c}}\|^2 = \text{const}$. This proves, that the curve is parameterized by a constant multiple of arc length. Moreover, it shows that $\ddot{\mathbf{c}}$ represents the principal curve normal, and orthogonality of the principal normal to Φ characterizes a geodesic. Note that the functional E_1 also optimizes the parameterization of the geodesic.

2.1 Computation of geodesics

According to [Struik 1950] the history of geodesics begins with Johann Bernoulli who first solved in 1697 the problem of computing the shortest distance between two points on a convex surface. Following Bernoulli also Euler studied geodesics and derived the equations for implicit surfaces in 1732. Classical differential geometry teaches us that we can always find a geodesic through a given surface point in a given tangent direction. This initial value problem can be solved by computing the solution of a system of first order ordinary differential equations. However, in applications one often asks for a geodesic that connects two specified surface points which leads to a much harder to solve boundary value problem.

A variety of applications of geodesics has been described within Computer Vision and Image Processing (see e.g. [Sapiro 2001; Osher and Paragios 2003; Kimmel 2003]). The type of surfaces we work on goes beyond parametric surfaces [Pham-Trong et al. 2001] and sometimes we are satisfied with approximately shortest curves. In Computer Graphics often triangle meshes are the preferred surface representation. For graphs the classical algorithm to compute shortest paths is the Dijkstra algorithm [Dijkstra 1959]. How-

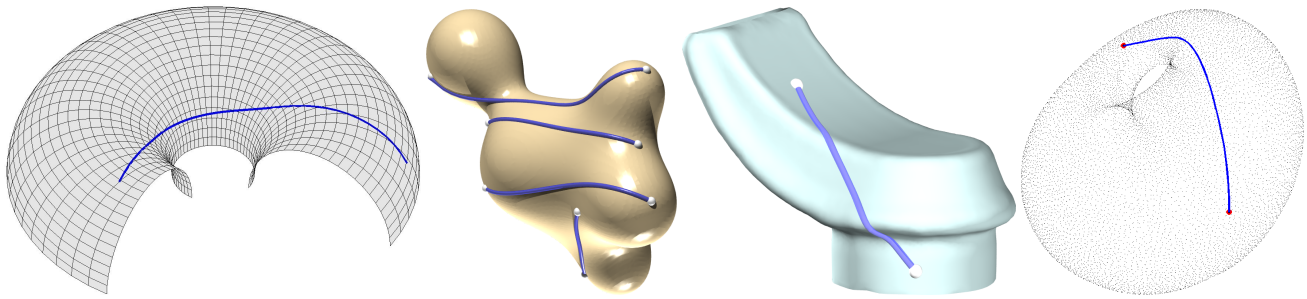


Figure 1: Geodesics on a parametric and implicit surface, a triangle mesh and a point set surface.

ever, for triangles meshes the shortest paths usually cut across faces and thus we can not simply use an edge-based Dijkstra algorithm. [Kimmel and Sethian 1998] employ a variant of the fast marching method to propagate the distance function on triangle meshes. By backtracking in negative gradient direction of the distance function one can then compute geodesic paths. A series of follow-up contributions [Novotni and Klein 2002; Kirsanov 2004; Reimers 2004] explored an improved update rule for geodesic computation. The original idea was also extended to weighted distance functions by [Bartesaghi and Sapiro 2001] which allows the computation of weighted geodesic curves. Thereby the weight depends e.g. on the mean surface curvature. With that approach shortest curves lying in areas of extremal surface curvature can be computed. The weighted approach was also extended to implicit hyper-surface [Mémoli and Sapiro 2001]. [Surazhsky et al. 2005] presented an efficient implementation of the exact geodesic algorithm by [Mitchell et al. 1987] which allows the computation of a geodesic from a single source point to one or many other points. The authors also extended the original algorithm to obtain on triangle meshes approximate geodesics with bounded error.

The algorithm of [Hofer and Pottmann 2004] minimizes the energy E_1 of Equ. (1). The method allows the computation of geodesic curves on parametric and implicit surfaces, triangle meshes and also on point set surfaces (Fig. 1). One advantage of that algorithm is that the surfaces can have arbitrary dimension and codimension which allows e.g. to employ the algorithm also for motion design purposes [Pottmann et al. 2004].

2.2 Geodesics with constraints

Often we are interested in the computation of shortest paths in the presence of obstacles. This problem has been extensively studied in robotics for motion design purposes [Halperin et al. 1997; Latombe 2001]. Motion design algorithms often assume that the obstacles have a polygonal shape. A possible solution for the computation of shortest planar (or spatial) curves connecting two points in the presence of arbitrarily shaped obstacles is the following [Hofer and Pottmann 2004]: From one of the two points we propagate the distance field using an adapted fast sweeping algorithm of [Zhao 2004]. The modification of the original algorithm is that grid nodes inside obstacles get a flag and are not used for the propagation. In Fig. 2 we illustrate level sets of the distance function in the presence of the two obstacles. Then a constrained geodesic is computed as described in [Hofer and Pottmann 2004]. The same approach can also be employed in 3D. An extension to geodesics on surfaces that avoid given obstacles (e.g. trimmed regions) can be achieved by adapting the fast marching method mentioned above such that again the distance field computation avoids the present obstacles.

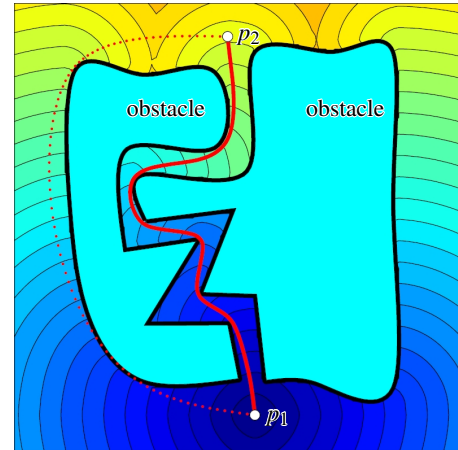


Figure 2: A planar geodesic curve connecting p_1 and p_2 constrained by two obstacles is shown as a solid line. The level sets of the constrained distance field to the point p_1 are color coded. Another longer path connecting p_1 and p_2 is shown as a dotted line.

3 Splines on surfaces

Curve design using splines is a fundamental topic in Computer Aided Geometric Design. B-spline curves of odd degree and maximal smoothness also arise as solutions of variational problems. In extension of standard spline methods, variational curve design has been investigated in many contributions (see e.g. [Brunnet et al. 1993; Moreton and Sequin 1993] and the references therein). Thus it is rather surprising that there are fewer contributions on the variational design of spline curves that are restricted to surfaces. [Shoemake 1985] introduced spherical counterparts of Bézier curves by extending de Casteljau's algorithm to the sphere. He replaced straight line segments by geodesic arcs and ratios of Euclidean distances by ratios of geodesic distances. Using this on the 3-sphere in \mathbb{R}^4 he generated the spherical component of rigid body motions and applied it to Computer Animation.

Motivated by the application to motion design, [Park and Ravani 1995] defined Bézier curves on Riemannian manifolds. Actually, a number of papers dealing with variational design on surfaces is considering the sphere [Brunnett and Crouch 1994; Brunnett et al. 1995], partially in view of the application to motion design [Park and Ravani 1997; Ramamoorthi and Barr 1997]. An early contribution to variational curve design on more general surfaces is by [Noakes et al. 1989]. The authors characterize the minimizers of an intrinsic geometric counterpart to the L^2 norm of the second deriva-

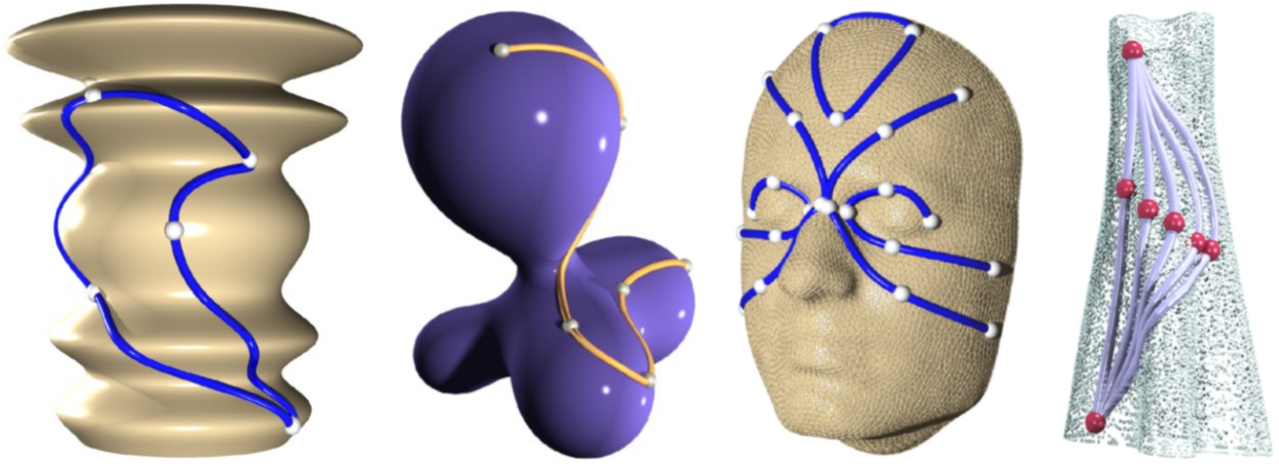


Figure 3: Energy minimizing spline curves on a parametric surface, a level set surface, a triangle mesh, and a point set surface.

tive. This is the integral of the squared covariant derivative of the first derivative with respect to arc length. Opposed to this intrinsic formulation there are also more recent contributions about splines in surfaces that deal with the usual energy functional employed in CAGD. This extrinsic formulation appears e.g. in the PhD thesis [Bohl 1999] for surfaces in \mathbb{R}^3 . Bohl proved the existence of a solution and illustrates computed examples based on a quasi-Newton optimization algorithm.

The counterparts on surfaces to C^2 cubic splines (and also the counterparts to splines in tension, C^4 quintic splines, and smoothing splines) have been characterized by [Pottmann and Hofer 2005]. In the unrestricted case the minimizers of the L^2 norm of the second derivative have cubic segments (vanishing fourth derivative). The corresponding splines on surfaces have segments with vanishing tangential component of the fourth derivative. More formally, in the unrestricted case we have the following result: Among all curves $\mathbf{x}(u) \subset \mathbb{R}^n$, whose first and second derivative satisfy $\dot{\mathbf{x}} \in AC(I)$, $\ddot{\mathbf{x}} \in L^2(I)$ on $I = [u_1, u_N]$, and which interpolate the given data, $\mathbf{x}(u_i) = \mathbf{p}_i$, the unique minimizer of

$$E_2(\mathbf{x}) = \int_{u_1}^{u_N} \|\ddot{\mathbf{x}}(u)\|^2 du, \quad (2)$$

is the interpolating C^2 cubic spline $\mathbf{c}(u)$. This well-known result has been extended by [Pottmann and Hofer 2005] to the case where the admissible curves $\mathbf{x}(u)$ are restricted to the given surface Φ . The energy functional E_2 of Equ. (2) is unchanged, but since the interpretation of E_2 requires an embedding space the restriction to a surface is seen as a constraint. The main theorem on the counterparts to interpolating cubic splines of [Pottmann and Hofer 2005] is

Theorem 1 Consider real numbers $u_1 < \dots < u_N$ and points $\mathbf{p}_1, \dots, \mathbf{p}_N$ on an m -dimensional C^4 surface Φ in Euclidean \mathbb{R}^n . We let $I = [u_1, u_N]$. Then among all C^1 curves $\mathbf{x} : I \rightarrow \Phi \subset \mathbb{R}^n$, which interpolate the given data, i.e., $\mathbf{x}(u_i) = \mathbf{p}_i$, $i = 1, \dots, N$, and whose restrictions to the intervals $[u_i, u_{i+1}]$, $i = 1, \dots, N-1$ are C^4 , a curve \mathbf{c} which minimizes the functional E_2 of Equ. (2) is C^2 and possesses segments $\mathbf{c}|_{[u_i, u_{i+1}]}$, whose fourth derivative vectors are orthogonal to Φ . Moreover, at the end points $\mathbf{p}_1 = \mathbf{c}(u_1)$ and $\mathbf{p}_N = \mathbf{c}(u_N)$ of the solution curve, the second derivative vector is orthogonal to Φ .

For a proof we refer the reader to the paper [Pottmann and Hofer 2005]. A linear combination of the energies (1) and (2) leads in the

unrestricted case to the well-known *splines in tension* as minimizers [Schweikert 1966]. The counterpart on surfaces is characterized by the following theorem of [Pottmann and Hofer 2005]:

Theorem 2 Consider a sequence of data points, parameter values and admissible curves on a surface Φ as in Theorem 1. Then, a minimizer of the functional

$$E_t(\mathbf{x}) = \int_{u_1}^{u_N} (\|\dot{\mathbf{x}}\|^2 + w\|\ddot{\mathbf{x}}\|^2) du, \quad w = \text{const} > 0, \quad (3)$$

is a C^2 curve which satisfies

$$tpr(\mathbf{c}^{(4)}(u) - w\ddot{\mathbf{c}}(u)) = 0 \quad (4)$$

on all segments. Thereby tpr denotes the orthogonal projection of a vector at a point $\mathbf{p} \in \Phi$ onto the tangent space of Φ at \mathbf{p} . The end conditions are $tpr\dot{\mathbf{c}}_+(u_1) = tpr\dot{\mathbf{c}}_-(u_N) = 0$.

3.1 Computation of splines on surfaces

In [Hofer and Pottmann 2004] a geometric optimization algorithm for the computation of energy-minimizing spline curves on surfaces is described. In the following we summarize the main ideas. We are minimizing *quadratic functionals* such as E_2 or E_t . After discretization we obtain *quadratic functions*. The restriction of the curves to a surface yields constraints, and thus the numerical computation of splines in manifolds requires an algorithm for the constrained minimization of a quadratic function. For this purpose we propose a projected gradient algorithm, whose step size control is guided by a geometric interpretation of an error estimate. Consider minimization of a quadratic function

$$F : \mathbb{R}^D \rightarrow \mathbb{R}, \quad F(\mathbf{x}) = \mathbf{x}^T \cdot \mathbf{Q} \cdot \mathbf{x} + 2\mathbf{q}^T \cdot \mathbf{x} + q,$$

with a symmetric positive definite matrix \mathbf{Q} , under the constraint that \mathbf{x} lies in some surface $\Phi \subset \mathbb{R}^D$. We assume that Φ has dimension m and that it is smooth in the area we work in.

The geometric approach to this minimization problem views the matrix \mathbf{Q} as matrix of the inner product $\langle \mathbf{x}, \mathbf{y} \rangle := \mathbf{x}^T \cdot \mathbf{Q} \cdot \mathbf{y}$, of a Euclidean metric in \mathbb{R}^D . F assumes its minimum in the point $\mathbf{p} = -\mathbf{Q}^{-1} \cdot \mathbf{q}$. Up to an unimportant additive constant, F then equals

$$F(\mathbf{x}) = (\mathbf{x} - \mathbf{p})^T \cdot \mathbf{Q} \cdot (\mathbf{x} - \mathbf{p}).$$

This is the squared distance $\|\mathbf{x} - \mathbf{p}\|^2$ of points \mathbf{p} and \mathbf{x} in the Euclidean norm mentioned above. Here, and in this entire section, ‘distance’, ‘orthogonality’, and related concepts refer to the metric defined by the matrix Q . The minimum of F on the surface Φ is attained at the point \mathbf{p}^* , which is closest to \mathbf{p} . \mathbf{p}^* is the normal footpoint of \mathbf{p} on Φ .

We propose the following iterative procedure for minimizing F . It consists of repeated application of the following two steps: \mathbf{x}_c (the current point) is initialized with an initial guess \mathbf{x}_0 for the minimizer.

1. Compute the tangent space T^m of Φ at the current iterate \mathbf{x}_c and project the point \mathbf{p} orthogonally into T^m , which results in the point \mathbf{p}_T .
2. Compute an appropriate stepsize s and project $\mathbf{x}_s := \mathbf{x}_c + s(\mathbf{p}_T - \mathbf{x}_c)$ onto Φ ; this yields the next iterate \mathbf{x}_+ .

For further details we refer the reader to [Hofer and Pottmann 2004].

3.2 Splines with constraints

Using the algorithm of [Hofer and Pottmann 2004] one can compute counterparts to cubic splines and splines in tension on surfaces in various representations (parametric, implicit, triangle mesh, point set surface), see Fig 3. Furthermore, their algorithm can be employed for variational curve design in the presence of obstacles [Hofer 2004; Hofer and Pottmann 2004] outlined below. Figure 4 illustrates planar and spatial spline curves that avoid given obstacles. Aimed at an application in computational anatomy energy-minimizing splines on surfaces were also extended to a weighted scheme in [Kao et al. 2007].

Only recently researchers in Computer Aided Geometric Design (CAGD) began to study the computation of spline curves in the presence of obstacles. In his PhD thesis, Bohl [Bohl 1999] presented an algorithm for the computation of energy-minimizing splines on trimmed two-dimensional parametric surfaces. More general results on the existence of energy minimizing splines in manifolds are due to Wallner [Wallner 2004]. Recently, Peters introduced SLEVEs for planar spline curves [Peters and Wu 2004] to solve the so-called ‘channel problem’ [Myles and Peters 2005]: Compute a spline curve with a limited amount of pieces that traverses a narrow channel bounded by polygonal obstacles. An older contribution by Opfer and Oberle [Opfer and Oberle 1988] dealt with cubic splines and obstacles and the constraint interpolation with rational cubics was studied by Meek et al. in [Meek et al. 2003]. [Hildebrandt et al. 2005] proposed an algorithm for smoothing 3d curves with an ε -constraint that keeps the curve inside a pipe surface of radius ε around the original curve.

Concerning the representation of obstacles the following approaches have been suggested so far. The paper [Azariadis and Aspragathos 2005] uses ‘bump-surfaces’ to represent obstacles. In our own work [Hofer and Pottmann 2004], we have used a single barrier manifold to represent all obstacles. Using that manifold we were able to compute energy minimizing splines that interpolate given points and avoid the obstacles as outlined above.

4 Variational motion design

The design of smooth motions of a rigid body in \mathbb{R}^3 is one of the most prominent applications of splines in manifolds. Many contributions to motion design use the quaternion unit sphere as a model

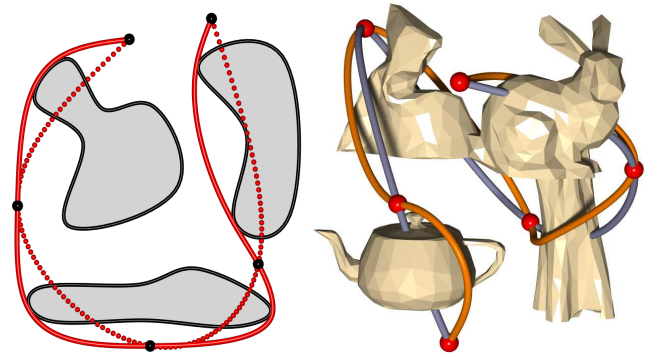


Figure 4: Variational curve design in the presence of obstacles in the (left) planar and (right) spatial case. Both figures also show the unrestricted cubic spline curve.

of $SO(3)$ (see e.g. [Shoemake 1985; Barr et al. 1992; Ramamoorthi and Barr 1997]). Nevertheless, one can also consider the group of Euclidean congruence transformations as a surface [Belta and Kumar 2002; Hofer et al. 2003] and base motion design on that surface. For that purpose [Hofer and Pottmann 2004; Pottmann et al. 2004; Hofer 2004] consider a rigid body moving in \mathbb{R}^3 . we use Cartesian coordinates and denote points of the moving system Σ^0 by $\mathbf{x}^0, \mathbf{y}^0, \dots$, and points of the fixed system by \mathbf{x}, \mathbf{y} , and so on. A rigid body transformation α maps points $\mathbf{x}^0 \in \Sigma^0$ to positions \mathbf{x} in the fixed system via

$$\mathbf{x} = \mathbf{a}_0 + A \cdot \mathbf{x}^0. \quad (5)$$

We speak of the image also as ‘position’ Σ ; it is determined by the pair (\mathbf{a}_0, A) , consisting of a vector \mathbf{a}_0 (the position of the origin) and the rotation matrix A . If $\mathbf{a}_0(u)$ and $A(u)$ depend smoothly on u , which can be thought of as time, we speak of a smooth motion, or sometimes simply of a motion. Our goal is the design of motions which interpolate given positions $\Sigma(u_i)$ at time instances u_i .

If we do not impose any restriction on the matrix A in (5), we get an *affine map* $\alpha(u)$ and an *affine position* $\Sigma(u)$. Let us denote the three column vectors of A as $\mathbf{a}_1, \mathbf{a}_2, \mathbf{a}_3$. Now we associate with the affine map α a point in 12-dimensional affine space \mathbb{R}^{12} , represented by the vector $\mathbf{A} = (\mathbf{a}_0, \dots, \mathbf{a}_3)$. Because of the orthogonality condition imposed on A , the image points of rigid body transformations α lie in a 6-dimensional manifold $M^6 \subset \mathbb{R}^{12}$.

A meaningful *metric* in \mathbb{R}^{12} can be introduced by means of a collection X of points $\mathbf{x}_1^0, \mathbf{x}_2^0, \dots, \mathbf{x}_K^0$ in the moving system (body), which are called *feature points*. The squared distance $\|\alpha - \beta\|^2$ of affine mappings α and β from each other is defined as sum of squared distances $\sum_i \|\alpha(\mathbf{x}_i^0) - \beta(\mathbf{x}_i^0)\|^2$ of the corresponding feature point positions. One does not have to use unit point masses at a discrete number of feature points. Instead, we could work with another mass distribution (positive measure) on the moving body.

It can be shown (see e.g. [Hofer et al. 2003]) that this distance measure introduces a Euclidean metric in \mathbb{R}^{12} , which only depends on the barycenter $\mathbf{s}_x = (1/K) \sum_i \mathbf{x}_i^0$ and on the inertia matrix

$$J := \sum_i \mathbf{x}_i^0 \cdot \mathbf{x}_i^{0T} \quad (6)$$

of the feature points. By a well-known result from mechanics, we can replace the set of feature points by the six vertices of their inertia ellipsoid, without changing the barycenter and the inertia matrix of X . To do so, we choose the barycenter as the origin in the moving system and the eigenvectors of J as coordinate axes. Then the six points have coordinates $(\pm f_1, 0, 0), (0, \pm f_2, 0), (0, 0, \pm f_3)$, where

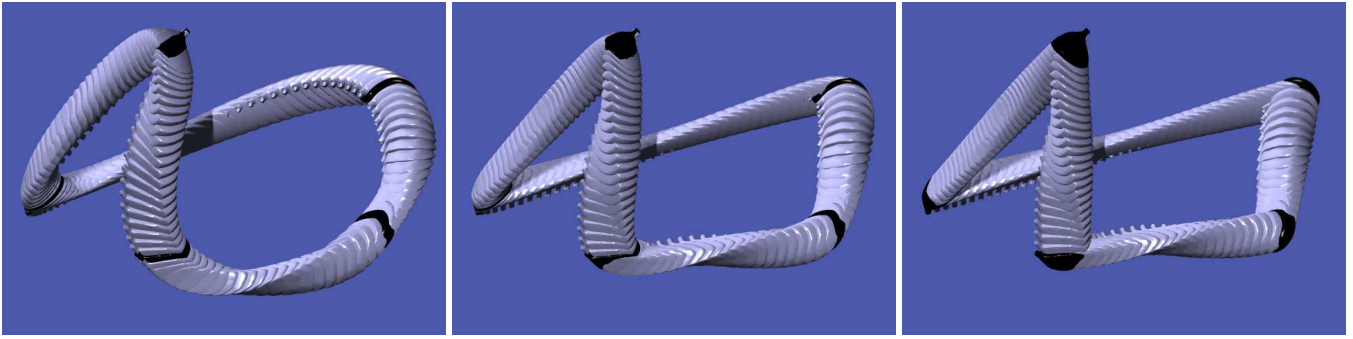


Figure 5: Energy minimizing cyclic motions: (Left) E_2 , (Center) E_t , (Right) E_1 .

$2f_i^2$ are the eigenvalues of J . Now, $\|\alpha - \beta\|^2$, i.e., the above defined squared distance of the points $\mathbf{A} = (\mathbf{a}_0, \dots, \mathbf{a}_3)$ and $\mathbf{B} = (\mathbf{b}_0, \dots, \mathbf{b}_3)$ from each other is given by the formula

$$\|\mathbf{A} - \mathbf{B}\|^2 = 6(\mathbf{a}_0 - \mathbf{b}_0)^2 + 2 \sum_{i=1}^3 f_i^2 (\mathbf{a}_i - \mathbf{b}_i)^2. \quad (7)$$

Variational motion design is seen as curve design with energy minimizing splines on $M^6 \subset \mathbb{R}^{12}$, using the metric (7). For motions, the meaning of minimizing one of the functionals E_1 , E_2 , or E_t , is that the total energy of the feature point trajectories is minimized. It makes sense to base motion design on trajectories of points on the moving body. We view this as an advantage over the known purely intrinsic formulations, which are neglecting shape and mass properties of the moving body. For the numerical solution we refer to [Hofer and Pottmann 2004]. An example of such motions is shown in Fig. 5. The same five input positions are interpolated by motions minimizing E_2 , E_t , and E_1 , respectively.

For a geometric characterization of the motions which are computed in this way [Pottmann et al. 2004] use the concept of a balanced force system from statics. A system of forces \mathbf{f}_i , attached to points \mathbf{p}_i , is in balance, if both, the sum of force vectors and the sum of moment vectors, vanish, i.e., $\sum_i \mathbf{f}_i = 0$, and $\sum_i \mathbf{p}_i \times \mathbf{f}_i = 0$. At an arbitrary time instant u of a sufficiently smooth motion, the k -th derivative vectors at the feature point positions define the k -th derivative force system \mathbf{S}_k . Now motions arising from the minimization of E_2 are characterized as follows: *The energy minimizing spline motion is C^2 , at each time instant $u \neq u_i$ the 4-th derivative force system $\mathbf{S}_4(u)$ is in balance, and at the end positions, the systems $\mathbf{S}_2(u_1), \mathbf{S}_2(u_N)$ of second derivatives are in balance. In particular, the trajectory of the barycenter of the feature points is an interpolating cubic C^2 spline.* For a proof, one uses the results of [Pottmann and Hofer 2005] and shows that the k -th derivative vector of a curve \mathbf{C} on M^6 at a point $\mathbf{C}(u)$ is orthogonal to M^6 if the k -th derivative force system of the corresponding position in \mathbb{R}^3 is in balance. The spline property of the barycenter trajectory follows immediately from (7) and the definition of E_2 ; therefore, the motion computation described above in \mathbb{R}^{12} can be decomposed into the computation of this special trajectory (in \mathbb{R}^3) and the computation of the rotational part (in \mathbb{R}^9).

4.1 Constrained motion design

Similar to the curve case one can perform motion design in the presence of obstacles [Hofer 2004; Hofer and Pottmann 2005] exploiting all available degrees of freedom. Figure 6 compares an unconstrained and a constrained (by four obstacles) energy-minimizing

rigid body motion interpolating five input positions. In recent work [Nawratil et al. 2007] present an algorithm that deals with rigid body motions and obstacles in a slightly different way. Motivated by a paper of [Zhang et al. 2006] a constrained geometric optimization algorithm for generalized penetration depth computation has been developed. Here the goal is to find the optimal motion that makes two colliding rigid bodies penetration free.

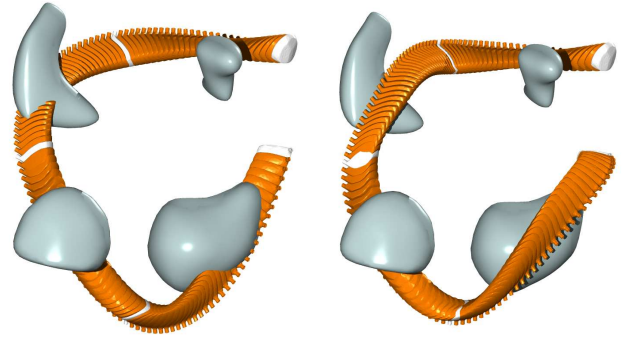


Figure 6: Variational motion design in the presence of obstacles. The energy-minimizing Euclidean rigid body motion (left) without constraints and (right) avoiding the given obstacles.

5 Fair webs

Fair webs have been described by [Wallner et al. 2007] and are energy-minimizing curve networks. Obtained via an extension of cubic splines or splines in tension to networks of curves, they are efficiently computable and possess a variety of interesting applications. Here we summarize properties of fair webs. Their discrete counterparts are fair polygon networks and both have interesting applications including fair surface design and approximation under constraints such as obstacle avoidance or guaranteed error bounds, aesthetic remeshing, parameterization and texture mapping, and surface restoration in geometric models.

While curve networks in 3-space are widely used and several contributions exist that use a variational approach, much less is known about energy-minimizing curve networks in surfaces, and in the presence of obstacles. Prior art on surface design based on energy-minimizing curve networks (without constraints) includes e.g. [Kolb 1995; Moreton and Sequin 1992]. In the discrete setting variational subdivision has been addressed in [Kobbelt and

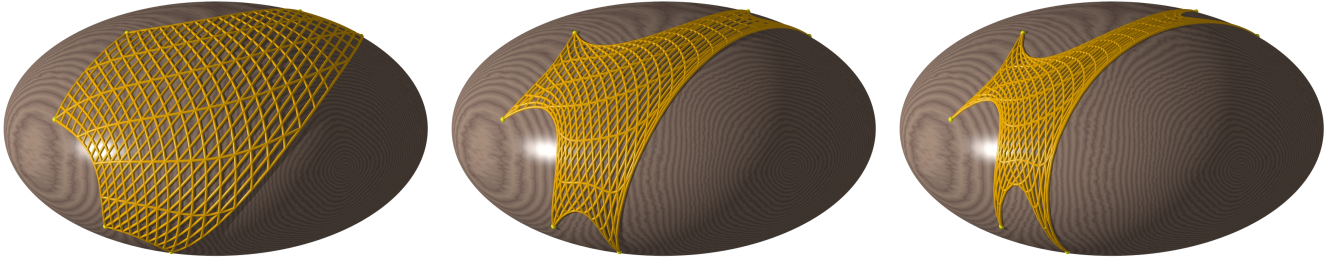


Figure 7: Curve networks on a surface which minimize an energy E . From left to right: $E = E_2$, $E = E_2 + 0.2E_1$, $E = E_1$. Fixed knots are marked by a ball. All other knots are free. The structure lines of the fair web reveal themselves beautifully.

Schröder 1998]. Note that there are also many contributions dealing with curve networks that do not explicitly use a variational approach and thus we do not cite those papers.

We summarize the main results from [Wallner et al. 2007]. A *curve network* is a finite set of curves $\mathcal{C} = \{c\}$, each defined in its parameter interval $[a_c, b_c]$. We call points which are common to more than one curve *knots*. One can think that the curves are being knotted together at the knots. Note that by “curve” we actually mean a curve segment between two knot points of the curve network. As in the familiar case of splines, some of these curves will later be joined to larger curves, called *structure lines*. Each *knot* k of the curve network has a collection C_k^s of curves *starting* there and another set C_k^e of curve segments *ending* there. The location of the knot in space is some point p_k . So if a curve c , defined in the interval $[a_c, b_c]$ starts in the knot p_k , i.e., $c \in C_k^s$, then $c(a_c) = p_k$, and analogously, if a curve c ends in the knot p_k , i.e., $c \in C_k^e$, then $c(b_c) = p_k$. The knots p_k together with the sets C_k^s , C_k^e define the *connectivity* of the network. Later on we will refer to the curves in the set C_k^s also as the *outgoing* curves of the knot p_k , and the curves in the set C_k^e as the *incoming* curves of p_k .

To obtain nice curve networks we often want that two curve segments joining in a knot (an incoming curve and an outgoing one) actually belong to one larger curve. More formally we state: a curve $c_e \in C_k^e$ ending in a knot p_k together with a curve $c_s \in C_k^s$ starting in p_k may be required to form a single smooth curve. These two curve segments (c_e, c_s) are part of what we call a *structure line* of the curve network. If two curves sharing a knot belong to a structure line, we say that these two curves have property (S). For a knot p_k , we collect all outgoing curves that have the property (S) in a set C_k^* . All outgoing curves $c \in C_k^*$ without property (S) are collected in a set C_k^{s*} , and the incoming curves $c \in C_k^e$ without property (S) form the set C_k^{e*} .

The energy of the entire curve network \mathcal{C} is the sum of energies of all single curves of the curve network:

$$E(\mathcal{C}) = \sum_{c \in \mathcal{C}} E(c). \quad (8)$$

Here E is either of E_1 , E_2 , or E_t . We refer to energy minimizing curve networks also as *fair* curve networks or short *fair webs*. Fair webs minimizing the energies E_2 , $E_1 + 0.2E_1$, and E_1 are shown in Fig. 7.

Fair webs constrained to surfaces have a number of nice properties. The most important from the fairness point of view is, that for E_2 - and E_t -minimizing fair webs, a structure line (which originally is required to be smooth only) is actually C^2 . Further, the derivatives of the curve segments which join in a free knot (whose location is not fixed as a side condition) fulfill some balance equations, which are detailed below. A discretized network (see [Wallner et al. 2007]) has analogous properties. We consider fair webs whose curves are

constrained to a given surface Φ . Although we assume that the connectivity of the fair web is maintained, we have the freedom to choose which knot points shall be *fixed* (their position is chosen, e.g. by the user), and which knot points shall be *free* (their position will be determined by the energy minimization procedure). In Fig. 7, fixed knots are marked.

We confine ourselves to C^2 curve segments in the case of E_1 and to C^4 segments in the case of E_2 and the tension energy E_t . A vector V attached to a point p in Φ can be written as $V = V^\top + V^\perp$, where V^\top is tangent and V^\perp is orthogonal to Φ in the point p . The vectors $c'(t), c''(t), \dots$ are attached to the point $c(t)$.

The main theorems in [Wallner et al. 2007] give a characterization of E -stationary curve networks for the different energies that we consider. We begin with the energy E_1 .

Theorem 3 E_1 -stationary curve networks in a surface Φ are characterized by:

- (i) The second derivative vectors c'' of all curves c are orthogonal to the surface Φ , i.e.,

$$c''^\top = 0$$

for all curves.

- (ii) For each free knot k ,

$$T_{1,k} := \sum_{c \in C_k^e} c'(b_k) - \sum_{c \in C_k^s} c'(a_k) = 0, \quad (9)$$

i.e., the first derivative vectors of incoming and outgoing curves are in equilibrium.

For curves in C_k^* which represent an incoming/outgoing pair and are therefore part of a structure line, the symbol $\Delta c''$ means the jump in c'' when leaving the incoming curve and continuing at the outgoing one, and similar for $\Delta c'''$. The next theorem describes curve networks which make the energy E_2 stationary.

Theorem 4 E_2 -stationary curve networks in a surface Φ are characterized by:

- (i) The fourth derivative vectors c'''' of all curves c are orthogonal to the surface Φ , i.e.,

$$c''''^\top = 0$$

for all curves.

- (ii) For each knot k , curves in C_k^{e*} and C_k^{s*} have $c''^\top = 0$ there, and the curves in C_k^* which are part of a structure line have $\Delta c'' = 0$ in the knot.

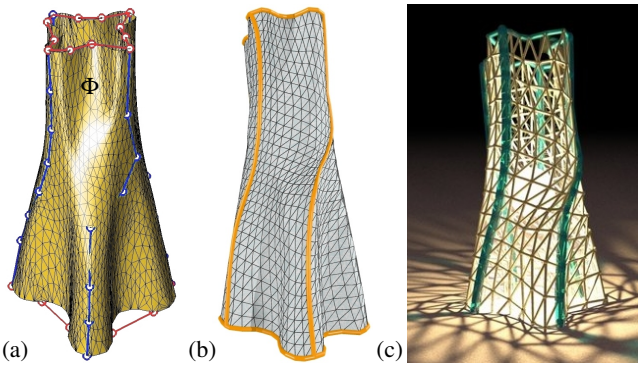


Figure 8: (a) User input on original mesh Φ are four polygons in vertical direction and two polygons in horizontal direction. (b) Fair mesh interpolating the input polygons. (c) Design based on coarser fair mesh interpolating the given polygons.

(iii) For each free knot k , $T_{2,k}^\top = 0$, where

$$T_{2,k} := \left(\sum_{c \in C_k^*} - \sum_{c \in C_k^*} \right) (c''^{\perp L} + c''') - \sum_{c \in C_k^*} \Delta c'''. \quad (10)$$

The following theorem gives a geometric characterization of E_t -stationary curve networks in a surface.

Theorem 5 For the tension energy $E_t = E_2 + tE_1$, E_t -stationary curve networks are characterized by:

(i) A linear combination of the fourth and the second derivative vector with the coefficients 1 and $-t$ vanishes,

$$(c'''' - tc'')^\top = 0$$

for all curves;

(ii) same as (ii) in Theorem 4;

(iii) at all free knots we have

$$(T_{2,k} - tT_{1,k})^\top = 0$$

where $T_{1,k}$ and $T_{2,k}$ are defined by Equ. (9) and Equ. (10) respectively.

For proofs of theorems 3,4,5 we refer the reader to [Wallner et al. 2007].

5.1 Constrained fair polygon networks

The discrete counterpart of fair webs are fair polygon networks. A wealth of possible applications of fair polygon networks is outlined in [Wallner et al. 2007]. In Fig. 8 we illustrate a remeshing example with user input that guides the structure lines of the new triangle mesh.

A special form of fair polygon networks turned out to be a useful tool for constrained smoothing of digital terrain elevation data [Hofer et al. 2006]. In the following we summarize the main ideas of the latter paper. Elevation data of the DTED-2 (Digital Terrain Elevation Data) specification are given as a height field over a uniform grid in the xy -plane, such that every data point has horizontal and vertical error (accuracy) bounds. Thus the error bounds are in the form of cylinders of revolution Z_{ij} (see Fig. 9). The objective is to compute a smooth surface that stays within the given

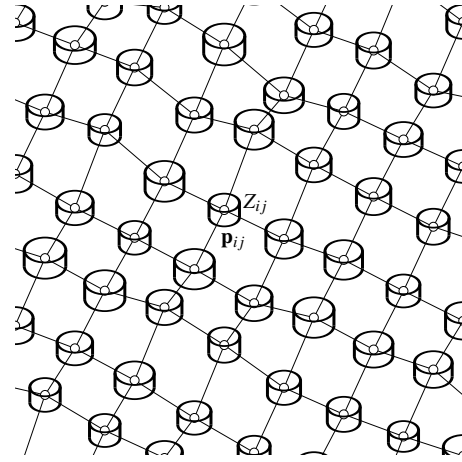


Figure 9: Smoothing height fields via fair polyline networks. Polyline network with the tolerance cylinders Z_{ij} associated with the vertices \mathbf{p}_{ij} .

error margins dictated by the cylinders. The framework proposed in [Hofer et al. 2006] views the height field over the xy -plane as a network consisting of x -parallel and y -parallel polylines. We perform smoothing by minimizing a discrete bending energy of these polylines, always respecting the error bounds. The framework is very flexible and allows e.g. to use individual error bounds for every data point, fill voids in the data, or smooth only a subset of the data for feature preservation.

The smoothing procedure of [Hofer et al. 2006] is based on minimizing the energy of a polyline network. We first define the energy of a single polyline, and then the energy of the polyline network as the sum of energies of all the polylines that contribute to the polyline network. A *polyline* $\mathbf{p} = (\mathbf{q}_1, \mathbf{q}_2, \dots, \mathbf{q}_L)$, as a discrete curve, possesses a discrete linearized bending energy:

$$E = \sum_{i=2}^{L-1} \|\Delta^2 \mathbf{q}_i\|^2, \quad \Delta^2 \mathbf{q}_i = \mathbf{q}_{i-1} - 2\mathbf{q}_i + \mathbf{q}_{i+1}. \quad (11)$$

Polyline networks have energies which are defined as the sum of the energies of the polylines which they are made of. The given elevation data constitute a rectangular array of points: $\mathbf{p}_{ij} = (x_{ij}, y_{ij}, z_{ij})$, ($i = 1, \dots, M$, $j = 1, \dots, N$). We define the energy of the data collection to be the sum of energies of the N different polylines defined by $j = \text{const.}$ and the M different polylines defined by $i = \text{const.}$:

$$E = \sum_{j=1}^N \sum_{i=2}^{M-1} \|\mathbf{p}_{i-1,j} - 2\mathbf{p}_{i,j} + \mathbf{p}_{i+1,j}\|^2 + \sum_{i=1}^M \sum_{j=2}^{N-1} \|\mathbf{p}_{i,j-1} - 2\mathbf{p}_{i,j} + \mathbf{p}_{i,j+1}\|^2. \quad (12)$$

A *fair* polyline network is one which has minimal energy among all networks which fulfill a fixed set of constraints.

The data sets we use consist of points \mathbf{p}_{ij} which are equally spaced in x and y direction. We might, without loss of generality, assume that $x_{ij} = g_x \cdot i$ and $y_{ij} = g_y \cdot j$, where g_x, g_y specify the grid element size (1 arc second for DTED-2). The data points contain errors, both in horizontal and vertical direction. If the horizontal error of a data point \mathbf{p}_{ij} is bounded by r_{ij} , and the vertical error by h_{ij} , then the true location of that data point is within a cylinder Z_{ij} of diameter $2r_{ij}$ and height $2h_{ij}$, which is centered in the given point $\mathbf{p}_{ij} = (x_{ij}, y_{ij}, z_{ij})$. Thus each point \mathbf{p}_{ij} is equipped with its own *tolerance cylinder* Z_{ij} (Fig. 9). They are hard constraints, which means that the terrain surface we are seeking has to pass through all Z_{ij} 's.

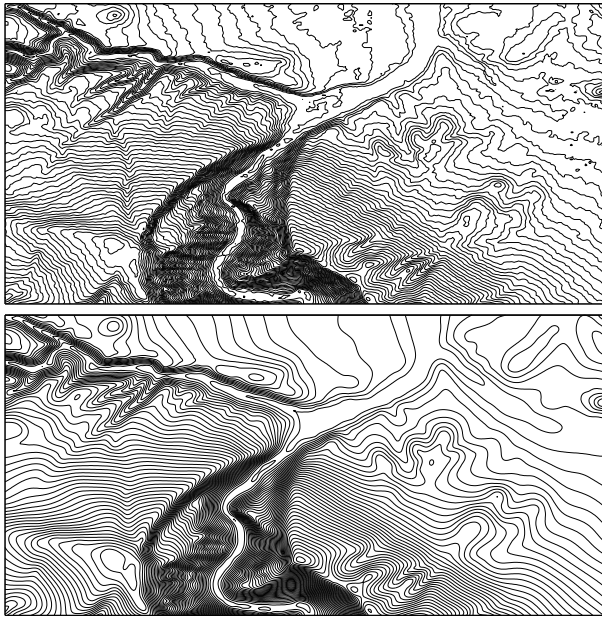


Figure 10: Iso-height contour plot of (top) original and (bottom) smoothed digital terrain elevation data. The constrained optimization procedure uses a fair polygon network.

Minimizing the quadratic function (12) of the variables x_{ij}, y_{ij}, z_{ij} , subject to the constraints mentioned above, is a quadratic programming problem with non-convex side conditions. It contains too many variables for just submitting it to a generic optimization procedure as, e.g., provided by mathematical software. [Hofer et al. 2006] showed that only using the z coordinates of the data points as variables for minimization is a meaningful approach:

$$E = \sum_{j=1}^N \sum_{i=2}^{M-1} (z_{i-1,j} - 2z_{i,j} + z_{i+1,j})^2 + \sum_{i=1}^M \sum_{j=2}^{N-1} (z_{i,j-1} - 2z_{i,j} + z_{i,j+1})^2. \quad (13)$$

A straightforward optimization scheme employs a gradient descent method, with the original elevation data as initial condition. It is elementary that the gradient of the energy is given by

$$(\nabla E)_{ij} = (z_{i-2,j} + z_{i+2,j} + z_{i,j-2} + z_{i,j+2}) - 4(z_{i-1,j} + z_{i+1,j} + z_{i,j-1} + z_{i,j+1}) + 12z_{i,j}, \quad (14)$$

provided $i, j > 2$ and $i < M - 1, j < N - 1$ (that is, we superimpose the masks $[1, -4, 6, -4, 1]$ in both x - and y -direction). As we approach the boundary, the standard mask becomes $[-2, 5, -4, 1]$ and finally $[1, -2, 1]$. Optimization is basically implemented as follows: First, we find a direction of descent, e.g., by letting $g_{ij} := -(\nabla E)_{ij}$. We consider the 1-parameter variation E_τ of the energy (13) defined by the z coordinates $z_{ij}(\tau) = z_{ij} + \tau \cdot g_{ij}$. The dependence of E on τ is quadratic, so it is easy to find a parameter $\tau = \tau_0$ where E_τ has a minimum. We replace z_{ij} by $z_{ij} + \tau_0 \cdot g_{ij}$, but vertices which have moved too far (violating the constraints) are pulled back. This procedure is iterated. Fig. 10 illustrates original and smoothed digital terrain elevation data by means of an iso-height contour plot. We see that the iso-height contour lines are much nicer after smoothing with our procedure but the digital terrain is still within the specified tolerances.

6 Conclusion

The recent progress made in the area of constrained optimization with energy-minimizing curves and curve networks helped to establish new theoretical results and a variety of practical applications. In the present survey paper we can only sketch the main results and thus we always refer to the original literature for detailed results. This interesting area of current research has proved to be a stimulating environment over the last few years and we hope that future contributions help to define this research area.

An extension of the research surveyed in the present paper is the following. Currently, conjugate curve networks on surfaces such as the principal curvature lines of relative differential geometry are proving themselves as fundamental tools for the generation of discrete freeform-surfaces with planar faces other than triangles. This theory in the hot field of discrete differential geometry has important applications in architecture that are currently under investigation.

Acknowledgements The research was supported by the Austrian Science Fund (FWF) under grants P18865-N13 and S92.

References

- AZARIADIS, P. N., AND ASPRAGATHOS, N. A. 2005. Obstacle representation by bump-surfaces for optimal motion-planning. *Robotics and Autonomous Systems* 51, 129–150.
- BARR, A. H., CURRIN, B., GABRIEL, S., AND HUGHES, J. F. 1992. Smooth interpolation of orientations with angular velocity constraints using quaternions. *Computer Graphics (Proceedings of ACM SIGGRAPH 92)*, 26, 2, 313–320.
- BARTESAGHI, A., AND SAPIRO, G. 2001. A system for the generation of curves on 3D brain images. *Human Brain Mapping* 14, 1–15.
- BELTA, C., AND KUMAR, V. 2002. An SVD-projection method for interpolation on $SE(3)$. *IEEE Trans. Robotics Automation* 18, 3, 334–345.
- BOHL, H. 1999. *Kurven minimaler Energie auf getrimmten Flächen*. PhD thesis, Univ. Stuttgart.
- BRUNET, G., HAGEN, H., AND SANTARELLI, P. 1993. Variational design of curves and surfaces. *Surv. Math. Ind.* 3, 1–27.
- BRUNETT, G., AND CROUCH, P. E. 1994. Elastic curves on the sphere. *Adv. Comput. Math.* 2, 23–40.
- BRUNETT, G., CROUCH, P., AND LEITE, F. S. 1995. Spline elements on spheres. In *Mathematical Methods for Curves and Surfaces*, Vanderbilt Univ. Press, M. Daehlen, T. Lyche, and L. Schumaker, Eds., 49–54.
- DIJKSTRA, E. W. 1959. A note on two problems in connexion with graphs. *Numerische Mathematik* 1, 269–271.
- DO CARMO, M. P. 1976. *Differential Geometry of Curves and Surfaces*. Prentice-Hall.
- HALPERIN, D., KAVRAKI, L., AND LATOMBE, J. C. 1997. Robotics. In *Handbook of Discrete and Computational Geometry*, J. E. Goodman and J. O'Rourke, Eds. CRC Press, New York, 775–778.
- HILBERT, D., AND COHN-VOSSEN, S. 1932. *Anschauliche Geometrie*. Springer Berlin.

- HILDEBRANDT, K., POLTHIER, K., AND PREUSS, E. 2005. Evolution of 3d curves under strict spatial constraints. *CAD-CG'05* 0, 40–45.
- HOFER, M., AND POTTMANN, H. 2004. Energy-minimizing splines in manifolds. *ACM Transactions on Graphics (Proceedings of ACM SIGGRAPH 2004)* 23, 3, 284–293.
- HOFER, M., AND POTTMANN, H. 2005. Designing energy-minimizing rigid body motions in the presence of obstacles. Tech. Rep. 142, Geometry Preprint Series, Vienna Univ. of Technology, July.
- HOFER, M., POTTMANN, H., AND RAVANI, B. 2003. Geometric design of motions constrained by a contacting surface pair. *Computer Aided Geometric Design* 20, 8–9, 523–547.
- HOFER, M., SAPIRO, G., AND WALLNER, J. 2006. Fair polyline networks for constrained smoothing of digital terrain elevation data. *IEEE Trans. Geosc. Remote Sensing* 44, 10/2, 2983–2990.
- HOFER, M. 2004. *Variational motion design in the presence of obstacles*. Phd thesis, Vienna University of Technology.
- KAO, C.-Y., HOFER, M., SAPIRO, G., STERN, J., REHM, K., AND ROTTENBERG, D. A. 2007. A geometric method for automatic extraction of sulcal fundi. *IEEE Trans. Medical Imaging* 26. to appear.
- KIMMEL, R., AND SETHIAN, J. 1998. Computing geodesic paths on manifolds. *Proc. of National Academy of Sciences* 95, 15 (July), 8431–8435.
- KIMMEL, R. 2003. *Numerical Geometry of Images: Theory, Algorithms, and Applications*. Springer.
- KIRSANOV, D. 2004. *Minimal discrete curves and surfaces*. Phd thesis, Harvard University.
- KOBBELT, L., AND SCHRÖDER, P. 1998. A multiresolution framework for variational subdivision. *ACM Trans. Graphics* 17, 4, 209–237.
- KOLB, A. 1995. *Optimierungsansätze bei der Interpolation verteilter Daten*. Phd thesis, Univ. Erlangen.
- LATOMBE, J. C. 2001. *Robot Motion Planning*, 6 ed. Kluwer.
- MEEK, D. S., ONG, B. H., AND WALTON, D. J. 2003. Constrained interpolation with rational cubics. *Computer-Aided Design* 20, 253–275.
- MÉMOLI, F., AND SAPIRO, G. 2001. Fast computation of weighted distance functions and geodesics on implicit hypersurfaces. *J. Comput. Phys.* 173, 2, 764.
- MITCHELL, J., MOUNT, D., AND PAPADIMITRIOU, C. 1987. The discrete geodesic problem. *SIAM Journal of Computing* 16, 4, 647–668.
- MORETON, H., AND SEQUIN, C. 1992. Functional optimization for fair surface design. In *ACM SIGGRAPH 92*, ACM, 167–176.
- MORETON, H., AND SEQUIN, C. 1993. Scale-invariant minimum-cost curves: fair and robust design implements. *Computer Graphics Forum* 12, 473–484.
- MYLES, A., AND PETERS, J. 2005. Threading splines through 3d channels. 139–148.
- NAWRATIL, G., POTTMANN, H., AND RAVANI, B. 2007. Generalized penetration depth computation based on kinematical geometry. Geometry Preprint 172, Vienna University of Technology, March.
- NOAKES, L., HEINZINGER, G., AND PADEN, B. 1989. Cubic splines on curved spaces. *IMA J. Math. Cont. & Inf.* 6, 465–473.
- NOVOTNI, M., AND KLEIN, R. 2002. Computing geodesic paths on triangular meshes. In *Proc. WSCG'02*, 341–348.
- OPFER, G., AND OBERLE, H. J. 1988. The derivation of cubic splines with obstacles by methods of optimization and optimal control. *Numer. Math.* 52, 17–31.
- OSHER, S., AND PARAGIOS, N. 2003. *Geometric Level Set Methods*. Springer, New York.
- PARK, F. C., AND RAVANI, B. 1995. Bézier curves on riemannian manifolds and lie groups with kinematic applications. *ASME J. of Mechanical Design* 117, 36–40.
- PARK, F. C., AND RAVANI, B. 1997. Smooth invariant interpolation of rotations. *ACM Transactions on Graphics* 16, 3, 277–295.
- PETERS, J., AND WU, X. 2004. SLEVES for planar spline curves. 615–635.
- PHAM-TRONG, V., SZAFRAN, N., AND BIARD, L. 2001. Pseudo-geodesics on three-dimensional surfaces and pseudo-geodesic meshes. *Numerical Algorithms* 26, 4, 305–315.
- POLTHIER, K., AND SCHMIES, M. 1998. Straightest geodesics on polyhedral surfaces. In *Mathematical Visualization*, Springer Heidelberg, K. P. H.C. Hege, Ed., 135–150.
- POTTMANN, H., AND HOFER, M. 2005. A variational approach to spline curves on surfaces. *Computer Aided Geometric Design* 22, 7, 693–709.
- POTTMANN, H., HOFER, M., AND RAVANI, B. 2004. Variational motion design. In *On Advances in Robot Kinematics*, J. Lenarčič and C. Galletti, Eds. Kluwer, 361–370.
- RAMAMOORTHI, R., AND BARR, A. 1997. Fast construction of accurate quaternion splines. In *Proceedings of ACM SIGGRAPH 1997*, ACM Press / ACM SIGGRAPH, New York, 287–292.
- REIMERS, M. 2004. *Topics in mesh based modeling*. Phd thesis, University of Oslo.
- SAPIRO, G. 2001. *Geometric Partial Differential Equations and Image Analysis*. Cambridge University Press.
- SCHWEIKERT, D. 1966. An interpolating curve using a spline in tension. *J. Math. Phys.* 45, 312–317.
- SHOEMAKE, K. 1985. Animating rotations with quaternion curves. *Computer Graphics* 19, 245–254. (Proc. SIGGRAPH'85).
- STRUIK, D. 1950. *Lectures on Classical Differential Geometry*. Addison-Wesley, Cambridge, MA.
- SURAZHISKY, V., SURAZHISKY, T., KIRSANOV, D., GORTLER, S. J., AND HOPPE, H. 2005. Fast exact and approximate geodesics on meshes. *ACM Trans. Graph.* 24, 3, 553–560.
- WALLNER, J., POTTMANN, H., AND HOFER, M. 2007. Fair webs. *The Visual Computer* 23, 1, 83–94.
- WALLNER, J. 2004. Existence of set-interpolating and energy-minimizing curves. *Computer Aided Geometric Design* 21, 883–892.
- ZHANG, L., KIM, Y., VARADHAN, G., AND MANOCHA, D. 2006. Generalized penetration depth computation. In *Proc. Symposium on Solid and Physical Modeling*, 173–184.
- ZHAO, H.-K. 2004. A fast sweeping method for eikonal equations. *Math. Comp.* 73.